research articles Journal of proteome research

Systems Biological Responses to Chronic Perfluorododecanoic Acid Exposure by Integrated Metabonomic and Transcriptomic Studies

Lina Ding,[†,‡,§] Fuhua Hao,[§,||] Zhimin Shi,[†] Yulan Wang,[||] Hongxia Zhang,[†] Huiru Tang,[*,||] and Jiayin Dai[*,†]

Key Laboratory of Animal Ecology and Conservation Biology, Institute of Zoology, Chinese Academy of Sciences, Beijing, 100101, People's Republic of China, State Key Laboratory of Magnetic Resonance and Atomic and Molecular Physics, Wuhan Centre for Magnetic Resonance, Wuhan Institute of Physics and Mathematics, Chinese Academy of Sciences, Wuhan 430071, People's Republic of China, and Graduate School of the Chinese Academy of Sciences, Beijing 100049, People's Republic of China

Received January 10, 2009

Perfluorocarboxylic acids (PFCAs) have been widely used in consumer and industrial products, such as food packaging, and found in the blood of both humans and wildlife. Although studies showed a high tendency toward biological accumulation and a variety of toxic effects for PFCAs, the mechanistic aspects of their toxicity remain unknown. In present study, we investigated the dosage-dependent metabonomic and transcriptomic responses of male rats to the exposure to perfluorododecanoic acid (PFDoA) over 110 days. Our NMR-based metabonomics results for both liver tissues and serum demonstrated that PFDoA exposure led to hepatic lipidosis, which was characterized by a severe elevation in hepatic triglycerides and a decline in serum lipoprotein levels. The results from transcriptomic changes induced by PFDoA corroborated these results with changes in gene transcript levels associated with fatty acid homeostasis. These results demonstrate that PFDoA induces hepatic steatosis via perturbations to fatty acid uptake, lipogenesis, and fatty acid oxidation. Several serum metabolites exhibited dose-dependences, providing thorough descriptions of changes induced by PFDoA exposure. These observations yielded novel insights regarding the toxicological mechanism of PFCAs at the systems level.

Keywords: hepatotoxicology • metabonomics • perfluorododecanoic acid • systems biology • toxicogenomics

Introduction

Perfluorododecanoic acid (PFDoA, $F(CF_2)_{11}CO_2$) is a member of the perfluorocarboxylic acids (PFCAs, $F(CF_2)_nCO_2$, $n \geq 7$) that have been used over the past 50 years in an increasing variety of consumer and industrial products, such as food packaging, fire-retardant foams, cosmetics, upholstery, surfactants, and surface protectors.[1] These compounds possess many useful characteristics for a range of applications, including resistance to degradation, thermal stability, and various surfactant properties. The ubiquitous presence of PFCAs in the environment has recently been discovered, and these compounds are present on a global scale in the blood of human populations[2,3] and wildlife.[4,5] Therefore, PFCAs have garnered intense scientific and regulatory interests due to their extraordinary persistence, bioaccumulation tendencies, and potential toxicological effects.[6,7]

PFCAs ($n \geq 7$) cannot be easily metabolized and excreted from the body; longer carbon chain PFCAs have higher accumulation capabilities and are more physiologically persistent than shorter chain PFCAs.[7–9] The toxic effects of PFCAs have already been observed in laboratory animals including body weight reduction, hepatotoxicity, tumorigenicity, immunotoxicity, and developmental toxicity.[10–12] A number of studies have demonstrated that the liver is the primary target organ of perfluorooctanoic acid (PFOA), which induces peroxisomal β-oxidation and inhibits the secretion of low-density lipoproteins and cholesterol from the livers of rodents.[3,13,14] Hepatic lesions, hepatocellular adenomas, and changes in hepatic peroxisomal palmitoyl-CoA oxidase have been reported in toxicity studies of PFOA and perfluorodecanoic acid (PFDA).[15–18] One prevailing hypothesis for the metabolic effects observed in laboratory animals in response to PFOA intoxication is that this compound is a ligand for the peroxisome proliferator-activated receptor-alpha (PPARα).[11] However, the evidence for PFOA as a PPARα ligand is unclear; PPARα knocked out mice still develop enlarged livers when fed PFOA, suggesting some other modes of action for this chemical. More recently, the PFDoA induced expression of PPARα and PPARγ, as well as target genes of these receptors, were also observed, resulting in significant hepatotoxicity in rats exposed to PFDoA for 14

* To whom correspondence should be addressed. Jiayin Dai: Tel: +86-(0)10-64807185, E-mail: daijy@ioz.ac.cn. Huiru Tang: Tel: +86-(0)27-87198430, Fax: +86-(0)27-87199291, E-mail: huiru.tang@wipm.ac.cn.
† Institute of Zoology.
‡ Graduate School of the Chinese Academy of Sciences.
§ These authors contributed equally to this work.
|| Wuhan Institute of Physics and Mathematics.

10.1021/pr9000256 CCC: $40.75
Published on Web 04/20/2009

days.[19] However, details regarding the mechanism of the PFCAs induced toxicity remain largely unknown.

Systems biology approaches, such as global gene expression profiling and metabonomics, are of great value for toxicological studies and have found widespread applications in obtaining a comprehensive understanding of the activity of various toxicants. However, gene expression changes at toxicological end points occur via a complex series of pathways, such as protein biosynthesis, protein modification, and metabolic alteration. Furthermore, biochemical changes do not always occur in the order of transcriptomic, proteomic, and then metabolic modifications. For instance, toxicological effects occurring at the metabolic level can induce subsequent adaptation at the proteomic or transcriptomic levels.[20] Therefore, genome-wide mRNA profiling only provides limited information regarding the action of PFCAs and is unable to predict changes in the metabolic profile in response to PFCA exposure. Metabonomics technology has shown great usefulness in understanding the toxin-induced endogenous metabolic responses and identifying the novel toxicity biomarkers.[21–23] Moreover, metabonomics approaches have theoretical advantages over genomic, transcriptomic, and proteomic ones since the metabolic network is downstream of gene expression and protein synthesis; thus, metabonomic investigations may reveal the cellular activity at a functional level.[24] Since metabolic biomarkers are closely associated with real biological end points and provide a global systems interpretation of biological effects, integration of metabolic and transcription profiles will provide greater reliability in explaining metabolic alterations caused by certain genes and allow for further elucidation of the toxicological effects and mechanisms of PFCAs.

In the present study, we conducted chronic PFDoA exposure (110 days) to better evaluate PFDoA hepatotoxicity to rats. NMR-based metabonomics were employed to investigate dose-dependent alterations in the metabolic profiles of serum, intact liver and liver extracts. Multivariate data analysis of the NMR spectra was then applied to discover endogenous metabolic changes after PFDoA treatment. To the best of our knowledge, this is the first study to investigate the alterations in gene expression caused by long-term PFDoA exposure combining the toxicogenomic and metabonomic analyses. The results will provide a comprehensive view of the toxicological mechanisms of PFDoA and allow for mapping of networks that define connectivity between gene expression and metabolite accumulation in rats. Furthermore, this systems biology approach will also provide critical information regarding the potential effects of such chemicals on human health.

Materials and Methods

Animal Experiments and Sample Collection. Male Sprague−Dawley rats (230−240 g) were obtained from Weitong Lihua Experimental Animal Central (Beijing, China). Animals were housed two per cage and maintained under a 12 h light-dark cycle at 20−26 °C with a relative humidity of 40−60%. Animals had access to food and water *ad libitum*. After one week of adaptation, the rats were randomly separated into five groups with 10 rats in each group including one control group and four treatment groups. The treatment groups were administered with PFDoA (CAS No.307−55−1, 95% purity, Sigma Aldrich, St. Louis, MO) suspended in 0.2% Tween-20 (Beijing Chemical Reagent Co. Beijing, China) orally via gavage for 110 days at doses of 0.02, 0.05, 0.2, and 0.5 mg/kg body weight/day. The dosages selected for this study were based on a prior acute experiment.[25] The body weights of the rats were recorded each day, and food consumption was measured twice weekly during the study. All rats were sacrificed after 110 days. Half of the liver was fixed in 2.5% formaldehyde and the other half and serum were immediately collected, frozen in liquid nitrogen, and stored at −80 °C.

Histopathology and Biomedical Analyses. To investigate the hepatic histopathological changes in PFDoA-exposed rats, glutaraldehyde-fixed liver slices were stained with hematoxylin and eosin (H&E) and examined by light microscopy.

Standard spectrophotometric methods for the HITAC7170A automatic analyzer were used to measure the following serum parameters: total bilirubin (T-Bil), serum alanine aminotransferase (ALT), total bile acids (TBA), alkaline phosphatase (ALP), albumin (ALB), aspartate aminotransferase (AST), creatine kinase (CK), urea nitrogen (BUN), creatinine (Cr), high density lipid-cholesterol (HDL-C), total cholesterol (T-CHO), triglyceride (TG), low density lipid-cholesterol (LDL-C), and blood glucose (Glc). Differences between the control and the treatment groups were determined using a one-way analysis of variance (ANOVA). The calculation was based on discrimination significance between classes at the level of $p < 0.05$.

Sample Preparation for ^{1}H NMR Spectroscopy. Serum samples were prepared by addition of 200 μL of D_2O containing 0.9% NaCl to 400 μL of serum, followed by centrifugation at 10 000 rpm for 10 min. A total of 550 μL of supernatant was transferred into 5 mm NMR tubes.

Liver samples (10−15 mg) were packed individually into a 4 mm ZrO_2 rotor, with addition of D_2O to provide a field lock.

Liver tissue (∼300 mg) was homogenized in an ice/water bath, and 600 μL of 50% methanol/50% water was added. After 30 s of sonication three times, the homogenates were centrifuged at 13 000 rpm for 10 min at 4 °C and the supernatants were collected. This procedure was repeated three times, and the collected supernatants were lyophilized and reconstituted in 0.1 M Na^+-K^+ buffer (TSP 0.005%, 10% D_2O, pH 7.43) for NMR analysis.

^{1}H NMR Spectroscopy. The ^{1}H NMR spectra of serum samples were acquired on a Bruker AVIII800 MHz spectrometer equipped with triple resonance and an inverse detection probe (Bruker Biospin, Germany). The same analysis was achieved for liver extracts using a Bruker AVIII 600 MHz spectrometer with a cryogenic probe, while the ^{1}H HRMAS NMR spectra of intact liver tissues were recorded on a Varian INOVA-600 spectrometer with a Varian NANO probe at a MAS spinning rate of 2200 Hz. All experiments were performed at 298 K and the detail processes were given in Supporting Information. For resonance assignment purposes, ^{1}H−^{1}H Correlation Spectroscopy (COSY), Total Correlation Spectroscopy (TOCSY), and J-Resolved Spectroscopy (JRES) 2D NMR spectra were also acquired.[26–28]

NMR Data Processing and Analysis. All acquired FIDs were multiplied by an exponential function equivalent to a 0.5 Hz line-broadening factor prior to Fourier transformation. The NMR spectra were manually phased and corrected for baseline distortion using Topspin 2.0 software (Bruker-Biospin, Germany). The serum CPMG spectra were referenced to the methyl group of lactate at δ 1.33, and the spectral region of δ 0.5−9.5 was segmented into 3168 bins having a width of 0.003 ppm using AMIX (Bruker-Biospin, Germany). Regions at δ 5.18−4.66 were excluded to remove residue water signals. The liver MAS NMR spectra were referenced to the anomeric proton of the β-glucose resonance at δ 4.66 and reduced to 801 segments

over a range of δ 0.5−8.5 with a width of 0.03 ppm. The aqueous extract spectra were referenced to the TSP peak at δ 0.00. The integrals of these buckets included the region between δ 0.5−9.5, which was divided into regions having a width of 0.003 ppm for each segment. The regions of the spectrum removed from the aqueous liver extract spectra included water (δ 4.71−5.08) and residual methanol (δ 3.34−3.38). Each integral region was normalized to the total sum of the spectra prior to data analysis.

Principle Component Analysis (PCA) and Orthogonal-Projection to Latent Structure-Discriminant Analysis (O-PLS-DA) of the NMR spectral data were performed using Simca-P 11.0 software (Umetrics, Sweden). The metabolites associated with the group separations were indicated by the loadings and coefficients in the coefficient plots calculated by back transformation of the loadings.[29,30,47] Coefficients were color coded using MatLab with a script downloaded from http://www.mathworks.com/ with some in-house modifications.

RNA Isolation and Microarray Analysis. Total RNA was isolated from ten rat livers per group with Trizol Reagent (Invitrogen Corp., Carlsbad, CA), according to the manufacturer's instructions. The concentration and purity of the total RNA were determined by spectrophotometry, and the quality was determined by the integrity of 28 and 18 S rRNA. Two groups (control and 0.2 mg/kg/d PFDoA) were selected for GeneChip analysis based on moderate histological and clinical chemistry changes. Microarray analysis was performed by CapitalBio Corp (CapitalBio, Beijing, China). The Affymetrix Rat Genome 230 2.0 array containing 31,000 gene probes composed of 25-mer single stranded oligonucleotides was used to monitor changes in gene expression. A total of six chips were used with three chips for the control and 0.2- dosed group, respectively. Equal amounts of RNA of each group were randomly pooled as three biological samples (containing three, three, and four randomly selected individual rats). The details of microarrays analysis was given in Supporting Information. The log-transformed signal data obtained for all probes were array-wise normalized using Affymetrix Dchip 2006, followed by gene expression analysis using the PLS-DA strategy with SIMCA-P 11.0A. One-seventh cross-validation was applied to the models to ensure that they were not overfitted. CapitalBio Molecule Annotation System (MAS) V 4.0 were used for pathway analyses (http://bioinfo.capitalbio.com/mas).

Quantitative Real-Time PCR. qRT-PCR was performed to validate the data obtained in the microarray analysis and to measure the expression of selected genes from three other dosed groups in addition to the 0.2 mg/kg/d group. cDNA was synthesized using an oligo-(dT)15 primer (Promega, Madison, WI) and M-MuLV reverse transcriptase (New England Biolabs, UK), according to the manufacturer's instructions. The details of qRT-PCR amplification was described in Supporting Information. PCR primers (Table S1, Supporting Information) were designed using Primer Premier 5.0 software. The housekeeping gene β-actin was used as an internal control. The PCR amplification was conducted at 95 °C for 15 min, followed by 40 cycles of 94 °C for 5 s, 50 or 56 °C for 15 s, and 72 °C for 10 s. The relative mRNA levels of selected genes were calculated using the $2^{-\Delta\Delta Ct}$ method.[31] Values were reported as means ± standard error (SE). Statistical differences were determined by one-way ANOVA multiple range test. Statistical significance was indicated with * to state $p < 0.05$.

Results

Organ Weights. There were no significant differences in the body weights of rats after treatment with PFDoA for 110 days (shown in Table S2, Supporting Information) at the doses of 0.02, 0.05, and 0.2 mg/kg/d, whereas a significant body weight reduction (about 7.1%, $p < 0.01$) was observed at the dose of 0.5 mg/kg/d with the average body weight decreased more rapidly during 60−110 days postdose (Table S3, Supporting Information). The liver weights significantly increased by 12.7, 10.0, 18.3, and 12.1% in the 0.02-, 0.05-, 0.2-, and 0.5-dosed groups ($p < 0.05$), respectively, while the relative liver to body weight also showed marked increase by 11.7, 8.3, 20.8, and 20.9% compared to the controls, respectively ($p < 0.05$).

Histopathology and Clinical Chemistry Analysis. Lipid droplets and widespread disintegrated cell systems were observed in the 0.05-, 0.2-, and 0.5-dosed groups, and the lipid droplets were larger in the high-dosed compared to the low-dosed groups (Figure 1). However, there were no apparent changes in the 0.02-dosed group. In the 0.2- and 0.5-dosed groups, hydropic degeneration and steatosis was clearly observed, as well as swollen and vacuolated hepatocytes with the largest karyons in the 0.5-dosed group, implying more severe liver injuries. Therefore, long-term exposure to PFDoA clearly resulted in liver tissue perturbations.

The PFDoA-induced hepatotoxicity in rats was also indicated by the clinical serum chemistry data for T-Bil, TBA, ALP, ALB, CK, BUN, Cr, TG, LDL-C, and glucose (Table 1). The most significant alterations included the elevation in ALB and glucose levels in the treated groups. Significant increases in the levels of TBA, ALP, BUN, and Cr were also detected for the groups receiving a dosage of 0.2 and 0.5, whereas elevated levels of T-Bil were only observed in the 0.5-dosed group ($p < 0.05$). The concentrations of CK were only elevated in the 0.02- and 0.05-dosed groups ($p < 0.05$). The concentrations of LDL-C were decreased in the 0.02- and 0.05-dosed groups ($p < 0.05$) while the levels of TG decreased significantly in the 0.05-, 0.2- and 0.5-dosed groups ($p < 0.05$). Surprisingly, no significant changes were observed in the levels of ALT, AST, HDL-C, and T-CHO in the dosed groups (Table 1).

NMR Spectroscopy of Serum and Liver Tissue. The typical ^{1}H NMR spectra of serum (Figure 2A), intact liver tissue (Figure 2B), and liver extract (Figure 2C) obtained from a control rat. The metabolite resonances were assigned according to literature[32–34] and results from 2D NMR experiments (Table S4, Supporting Information). Serum spectra were comprised of mainly lipoprotein, glycoprotein, glucose, amino acids, carboxylic acids, creatine, and choline metabolites. NMR spectra of liver tissues were dominated by resonances from triglycerides, fatty acids, glucose, and glycogen while the NMR spectra of liver extracts were dominated by amino acid, carboxylic acid, and glutathione signals. No outliers were observed in all cases from PCA. In order to maximize the separation between data obtained from PFDoA-exposed and control rats and to obtain information on the metabolites significantly contributed to classifications, the O-PLS-DA models with unit variance scaling was subsequently performed (Figure 3, Table S5, Supporting Information).

Good separation between the ^{1}H NMR spectra of serum samples obtained from dosed rats and corresponding controls was achieved as shown in the O-PLS-DA cross-validated scores plots (Figure S1 A−D). Metabolites having significant contributions to the separation are evident in the corresponding

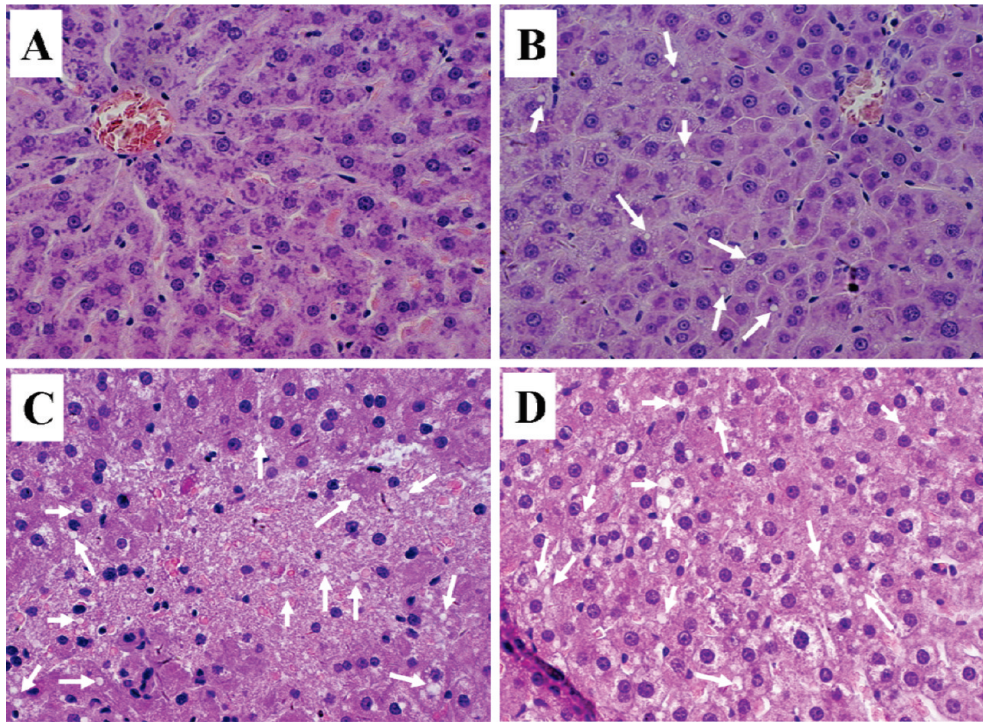

Figure 1. Hepatic histopathology. Light microscopy (×400) of (A) control, (B) 0.05 mg/kg/d, (C) 0.2 mg/kg/d, and (D) 0.5 mg/kg/d. Arrows indicate lipid droplets.

Table 1. Effect of PFDoA on Selected Clinical Chemistry Parameters

		PFDoA (mg/kg/d)			
parameters	control	0.02	0.05	0.2	0.5
T-CHO (mmol/L)	1.66 ± 0.09	1.58 ± 0.10	1.46 ± 0.10	1.52 ± 0.09	1.63 ± 0.12
HDL-C (mmol/L)	1.11 ± 0.08	1.12 ± 0.08	1.00 ± 0.09	1.06 ± 0.08	1.18 ± 0.07
LDL-C (mmol/L)	0.18 ± 0.02	0.13 ± 0.01*	0.13 ± 0.01*	0.16 ± 0.01	0.22 ± 0.02
TG (mmol/L)	2.10 ± 0.27	1.66 ± 0.09	1.53 ± 0.16*	0.89 ± 0.09**	0.50 ± 0.05**
Glucose (mmol/L)	7.82 ± 0.18	8.55 ± 0.14**	8.95 ± 0.22**	9.37 ± 0.24**	8.47 ± 0.14**
Cr (μmol/L)	67.6 ± 1.4	69.5 ± 1.1	70.9 ± 0.92	72.7 ± 1.60**	72.2 ± 0.83**
BUN (mmol/L)	6.32 ± 0.22	6.61 ± 0.25	6.91 ± 0.30	7.38 ± 0.25**	8.86 ± 0.35**
T-Bil (μmol/L)	1.00 ± 0.09	0.80 ± 0.06	0.85 ± 0.08	0.92 ± 0.04	1.08 ± 0.09*
TBA (μmol/L)	12.74 ± 2.16	6.17 ± 0.94	11.67 ± 2.25	19.98 ± 3.07**	20.58 ± 3.30**
ALT (U/L)	60.0 ± 4.4	71.0 ± 3.5	57.8 ± 3.3	70.2 ± 2.4	64.2 ± 4.7
AST (U/L)	137.5 ± 6.9	151.8 ± 6.3	154.0 ± 11.7	146.0 ± 5.9	142.9 ± 4.2
ALP (U/L)	140.1 ± 15.0	167.6 ± 10.8	144 ± 9.5	241.8 ± 9.8**	228.0 ± 14.2**
ALB (g/L)	31.91 ± 0.67	33.81 ± 0.35**	33.30 ± 0.35**	34.20 ± 0.54**	32.93 ± 0.44*
CK (U/L)	6428.9 ± 300.7	7903.3 ± 410.1*	8490.4 ± 948.7*	6749.9 ± 608.9	6338.6 ± 439.0

coefficient plot (Figure 3A), for the representative O-PLS-DA coefficient plot of the 0.5-dosed group (other dosed groups are shown in Figure S1E−G, Supporting Information). For this data, positive peaks indicate a decrease in the PFDoA-dosed rats. The color of the peaks indicates the significance of the metabolites contributing to the separation, with red being more significant than blue, as indicated in a color scaling map on the right-hand side of the coefficient plot. A coefficient of 0.7 was used as the cutoff value and was calculated based on discrimination significance at the level of 0.05 ($p < 0.05$). Significantly changed metabolites and their coefficients for different groups are shown in Table 2. The levels of lipoproteins and lipids in serum decreased significantly, while small molecules such as amino acids (Ile, Leu, Val, Ala, Lys, Phe, Tyr, Glu, Gln, and His), lactate, D-3-hydroxybutyrate, pyruvate, acetate, citrate, creatine, formate, and glucose increased dramatically in the serum of dosed animals. There were no significant metabolite alterations in the 0.02-dosed rats, and the 0.05-, 0.2-, and 0.5-dosed groups were remarkably different from the control (Table 2).

Good separation was also obtained between the dosed rats and controls in terms of their NMR spectra of intact liver and liver aqueous extracts, demonstrating a significant difference for the 0.05-, 0.2- and 0.5-dosed groups. In those groups, there are all clear separations compared to the control (Figures 3B, 3C and S2, S3, Supporting Information) The predominant variations in biochemical composition identified in the livers of dosed rats, in contrast to the composition observed in serum, included an increase in signal intensities from triglycerides and fatty acids. Additionally, the intensities of glucose, glycogen, trimethylamine-*N*-oxide (TMAO), glutamine, glutamate, and phospholipids together with choline were reduced in rats exposed to PFDoA (Figure 3B). The metabolites that were significantly changed in the 0.2 and 0.5-dosed groups and their corresponding coefficients are displayed in Table 2. Similar to liver tissue, significant changes in metabolites occurred mainly

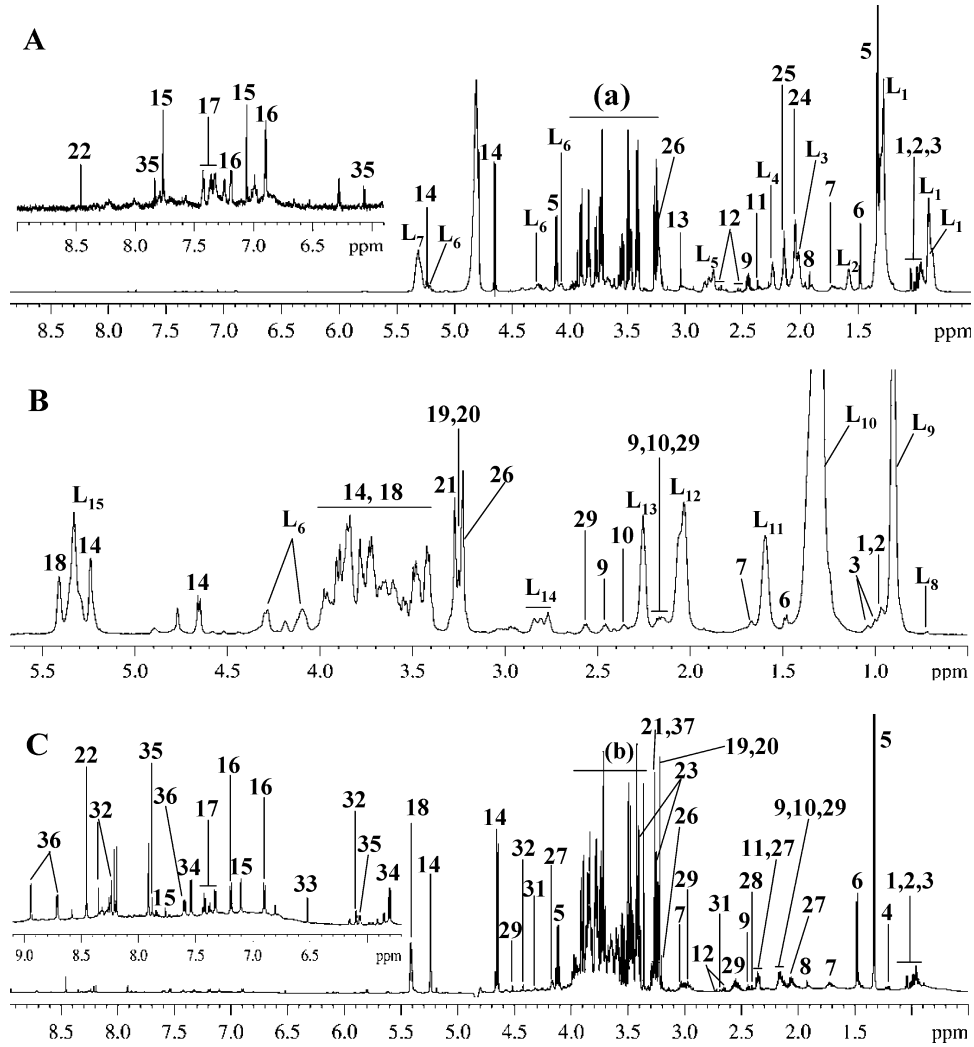

Figure 2. Representative ^{1}H NMR spectra of rat serum and liver samples from the control group: (A) 800 MHz ^{1}H CPMG spectra of serum; (B) 600 MHz ^{1}H MAS CPMG spectra of intact liver tissue; (C) 600 MHz ^{1}H NOESYGPPR 1D spectra of liver aqueous extracts. (a) Glucose and amino acid αCH resonances. (b) Glucose, glycogen, and amino acid αCH resonances.

in aqueous liver extracts of high-dosed rats (Figure 3C). The levels of glycine, proline, succinate, glutathione (GSSG), inosine, nicotinurate, and uracil, as well as phospholipid degradation products, such as choline, phosphorylcholine, and glycerophosphorylcholine were clearly elevated in the liver extracts of dosed rats. Additionally, the resonances corresponding to pyruvate, malate, glucose, glycogen, and taurine were clearly depleted in the dosed animals.

To validate the metabolic changes in the serum induced by PFDoA exposure and further explore the dependence of these changes on dosage, ratios of the NMR intensity of selective metabolites from dosed rat serum compared to the corresponding controls were calculated from 800 MHz ^{1}H NMR spectra of the diffusion-edited (Figure 4A) and CPMG subspectra (Figure 4B) ($n = 10$ for each group). The concentrations of unsaturated fatty acids (UFA), polyunsaturated fatty acids (PUFA), and CH_3, $(CH_2)_n$ moieties of lipoprotein lipid decreased as the dosage increased, whereas the levels of glucose, citrate, valine, isoleucine, and formate increased as the dosage increased, confirming the O-PLS-DA results.

Global Gene Expression Analysis. Good separation was obtained between the control and 0.2-dosed groups from PLS-DA model. The coefficients representing the 95% confidence interval were used as the criterion for significant changes. A total of 394 genes showed significant changes, with coefficients of more than 0.95 or less than −0.95 ($p < 0.5$). Furthermore, a q-value of less than 10% (the lowest False Discovery Rate) for a single gene is significant according to Affymetrix's manual. After exclusion of genes with q-values more than 10% among 394 affected genes, 280 genes remained, of which a total of 153 genes were up-regulated and 127 genes were down-regulated. After exclusion of genes lacking annotations, 115 up-regulated and 62 down-regulated genes were obtained (Table S6 and S7, Supporting Information). Significantly altered gene expression also included genes involved in the metabolism of carbohydrates and amino acids, apoptosis, transport, signal transduction, and proteolysis. Pathway analysis was further conducted according to the combination of KEGG pathways in the Kyoto Encyclopedia of genes and genomes (www.genome.ad.jp/keg) and GenMAPP organization (www.genmapp.org). Genes involved in fatty acid biosynthesis and beta-oxidation, including *Fads*, *Decr1*, *Acaa2*, *Acox1*, *Slc25a20*, *Decr2*, *Ech1*, *Hadhb*, *Acadv1*, *Acadm*, *Acadl*, *Ehhadh*, and *Abhd1*, were significantly up-regulated after exposure to PFDoA. Genes involved in the synthesis and degradation of ketone bodies, such as *Acat1* and *Hmgcs2*, also exhibited marked activation. *Cte1* and *Mte1*, which

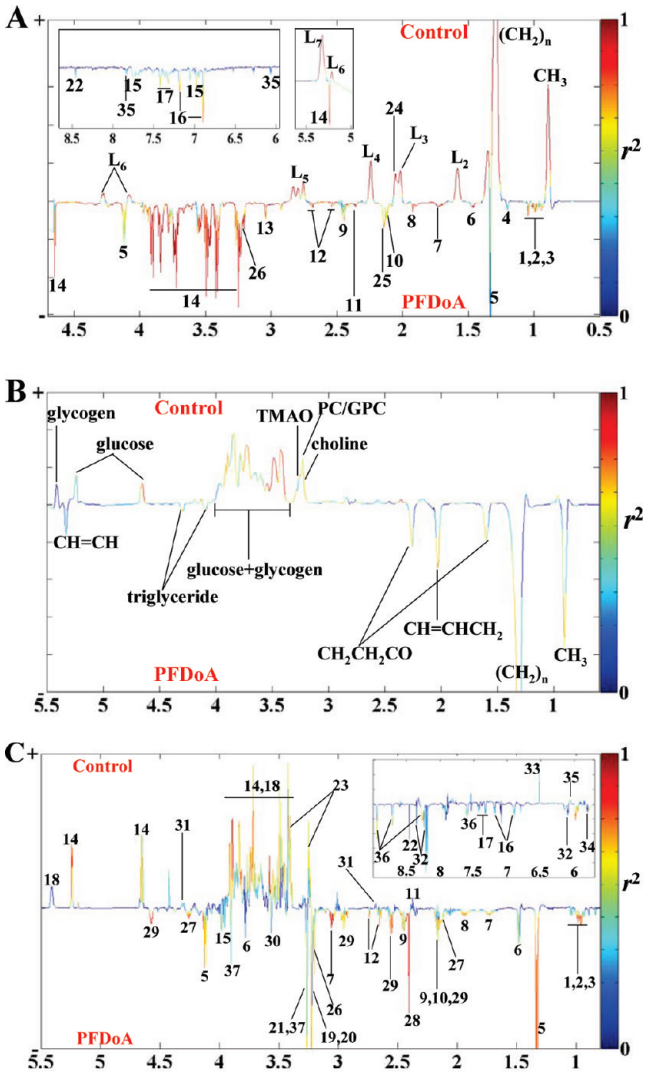

Figure 3. O-PLS-DA coefficient-loading plots for rats exposed to 0.5 mg/kg/d PFDoA compared to controls. (A) Serum data, (B) data for intact liver tissues, and (C) data for the hydrophilic liver extracts.

are key regulators of acyl-CoA metabolism, increased with the highest fold changes in this study. Genes involved in fatty acid transport, such as *Cd36*, *Adrp*, and *Crot*, were significantly induced after PFDoA treatment. A number of genes that participate in lipid metabolism and other biological processes demonstrated altered expression profiles (Table S6 and S7, Supporting Information). Among the most striking changes induced by PFDoA in rats were genes involved in xenobiotic metabolism, including those with phase I (oxidation), phase II (conjugation), and phase III (transport) functions. Phase I genes included members of the alcohol dehydrogenase (*Aldh1a1* and *Aldh1a7*), epoxide hydrolase (*Ephx2*), and cytochrome P450 (Cyp) families. Phase II genes included uridine diphosphate glucuronosyl transferase (*Ugt*). Phase III genes included members of the adenosine triphosphate-binding cassette transporter (*Abc*) and solute carrier (*Slc*) families (*slc22a5*, *slc25a20*, and *slc3a2*). The cytochrome groups are also of great interest since these genes are related to the metabolism of xenobiotics. *Cyp2b*, which is responsible for catalytic reactions involved in drug metabolism, was up-regulated 5.8-fold. *Cyp2j4*, which is a putative cytochrome p450 monooxygenase enzyme, was up-regulated by PFDoA. The *Cyp4a* family (*Cyp4a1*, *Cyp4a2*, *Cyp4a3*, and *Cyp4a8*) plays an important role in lipid metabolism and the detoxification of xenobiotics. Specifically, these isoenzymes catalyze the ω- and $\omega-1$ hydroxylation of fatty acids, including arachidonic acid, and the ω-hydroxylation of prostaglandins in the liver. The transcriptional expression of *Cyp4a1*, *Cyp4a2*, and *Cyp4a3* increased significantly by 5.6-, 1.5-, and 2.1-fold, respectively. However, *Cyp4a8* was down-regulated 12-fold by PFDoA exposure. In addition, *Cyp17a1*, which is responsible for steroid hydroxylation and comprises a main component of the steroidogenic pathway, was up-regulated 6-fold by PFDoA exposure.

To validate the microarray data, the mRNA expression of nine genes involved in lipid homeostasis was assessed by *q*RT-PCR analysis for all dosed groups (Figure 5). The *q*RT-PCR results demonstrated that the RNA levels of *PPAR*α (the signal was weak in GeneChip), a major regulator in hepatic fatty acid β-oxidation, were elevated 2.9-fold in the 0.2-dosed group and 4.6-fold in the 0.5-dosed group compared to the controls ($p < 0.05$). Furthermore, the expression of *PPAR*γ increased 2-fold and 3.2-fold in 0.2- and 0.5-dosed rats, respectively. The mRNA levels of *Hadhb*, *Acox*, *Cyp4a1*, and *Cd36*, the important target genes of *PPARs*, were significantly induced in the 0.2- and 0.5-dosed groups, being consistent with the induction of *PPAR*α. *Adrp* was significantly induced (by 3.4-fold) in the 0.5-dosed group. The mRNA levels of *Apom* and *Hsd11b1* decreased significantly in the 0.2- and 0.5-dosed groups, which exhibited consistent alterations by microarray analysis. The expression of these genes was not affected in the 0.02- or 0.05-dosed rats compared to the control group.

Discussion

The results presented herein validate that metabonomics coupled with genomic profiling provides detailed toxicological information for rats after chronic dosing with PFDoA. With the availability of powerful high-throughput and multiend point analysis tools, we can now obtain complete assessments of the functional activity of biochemical pathways involved in lipid homeostasis, as well as carbohydrate and amino acid metabolism, a previously unattainable endeavor. The systems biology approach has great potential for improving the way we understand biological information, which is not only applicable to toxicological research, but also utilizable to identify biomarkers for evaluating the risk of human PFCA exposure.

The elevated lipid concentrations in liver tissue as well as the decreased lipid and lipoprotein concentrations in serum demonstrated that alterations in lipid metabolism occurred as a result of PFDoA induced hepatotoxicity. Histopathological changes, such as obvious lipid droplets and steatosis in the liver, further identified the unbalanced lipid homeostasis induced by PFDoA. Moreover, gene expression changes involved in fatty acid metabolism also support the evidence that PFDoA disrupted lipid metabolism in rat liver. Therefore, these results demonstrated that PFDoA caused perturbations in lipid metabolism and resulted in injury to the rat liver following chronic PFDoA exposure.

PPARα and PPARγ are key regulators of lipid homeostasis and can be activated by a structurally diverse group of compounds. PPARs transactivate target genes upon binding to peroxisome proliferator-response elements (PPREs) through heterodimerization with another nuclear hormone receptor, retinoid X receptor (RXR).[35] However, the effects on signaling pathways downstream of PPARs remain unclear. PFCAs have

Table 2. Significantly Changed Metabolites in the Serum, Liver, and Liver Extracts of Male Rats Exposed to PFDoA from NMR Data[a]

		blood serum			liver tissue			aqueous extract		lipid extract	
no.	metabolites	dose1	dose2	dose3	dose1	dose2	dose3	dose2	dose3	dose2	dose3
L_1	lipoprotein	0.70	0.92	0.97							
L_7	triglyceride	0.75	0.96	0.98	−0.72	−0.88	−0.83			−0.90	−0.93
L_8	UFA	0.76	0.91	0.98	−	−0.68	−0.60			−0.96	−0.96
L_{16}	phospholipid									0.88	0.89
1	isoleucine	−0.81	−0.77	−0.94				−0.81	−0.60		
2	leucine	−0.80	−0.83	−0.91				−0.84	−0.85		
3	valine	−	−0.73	−0.89				−0.80	−0.82		
4	3-HB	−	−	−0.66				−	−		
5	lactate	−0.80	−0.87	−0.96				−0.68	−0.88		
6	alanine	−	−0.73	−0.73				−	−0.67		
7	lysine	−0.83	−0.88	−0.97				−0.82	−0.77		
8	acetate	−0.79	−0.80	−0.90				−0.76	−0.79		
9	glutamine	−0.77	−0.74	−0.75				−0.89	−0.90		
10	glutamate	−0.91	−0.88	−0.95				−0.91	−0.90		
11	pyruvate	−0.72	−0.93	−0.97				0.72	−		
12	citrate	−0.73	−0.85	−0.90				−0.81	−0.86		
13	creatine	−0.74	−0.72	−0.90							
14	glucose	−0.72	−0.91	−0.97	0.77	0.80	0.79	0.65	0.84		
15	histidine	−	−0.78	−0.81				−	−		
16	tyrosine	−	−0.90	−0.93				−0.76	−0.61		
17	phenylalanine	−0.83	−0.78	−0.90				−0.81	−0.82		
18	glycogen				0.64	0.73	0.65	0.80	0.85		
19	PC				0.83	0.80	0.76	−0.86	−0.94		
20	GPC				0.70	0.83	0.75	−	−0.75		
21	TMAO				0.69	0.80	0.80	−	0.73		
22	formate	−	−0.74	−0.61				−0.75	−		
23	taurine							0.70	0.84		
24	NAG	0.76	0.93	0.94							
25	OAG	−0.74	−0.67	−0.82							
26	choline	−0.69	−0.80	−0.95	0.73	0.78	0.74	−	−0.79		
27	proline										
28	succinate							−0.94	−0.95		
29	glutathione							−0.80	−0.83		
30	glycine							−0.66	−0.84		
31	malate							−	0.68		
32	inosine							−0.77	−0.81		
34	uracil							−0.60	−0.77		
35	uridine							−	0.77		
36	nicotinurate							−0.91	−0.86		
37	betaine							0.82	0.88		

[a] Dose 1, 0.05 mg/kg/d; Dose 2, 0.2 mg/kg/d; Dose 3, 0.5 mg/kg/d. PUFA, polyunsaturated fatty acid; UFA, unsaturated fatty acid; NAG, *N*-acetyl-glycoprotein; OAG, *O*-acetyl-glycoprotein; 3-HB, 3-hydroxybutyrate; TMAO, trimethylamine-*N*-oxide; PC, phosphorylcholine; GPC, glycerophosphorylcholine. The numbers mean the correlation coefficients of the related metabolites. Positive values indicate a decrease and negative values indicate an increase compared to control.

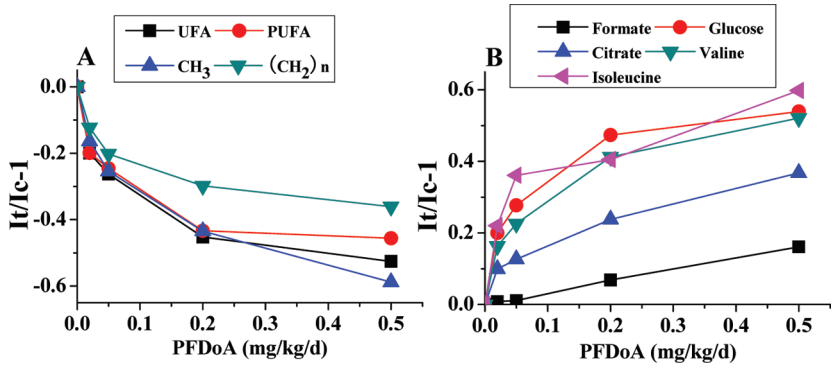

Figure 4. Dosage-dependence of NMR resonances derived from the ^{1}H NMR spectra of rat blood serum: (A) diffusion-edited NMR spectra and (B) CPMG spectra. It, Intensity of the PFDoA-treated rat; Ic, Intensity of the control rat; UFA, unsaturated fatty acids; PUFA, polyunsaturated fatty acids; CH_3, methyl group of the lipoprotein; CH_2, ethyl group of the lipoprotein.

a structure similar to that of endogenous fatty acids, except that fluorine atoms replace the hydrogen ones. Therefore, PFCAs could potentially be mistaken as a substrate by the fatty acid metabolism machinery due to structural similarity with

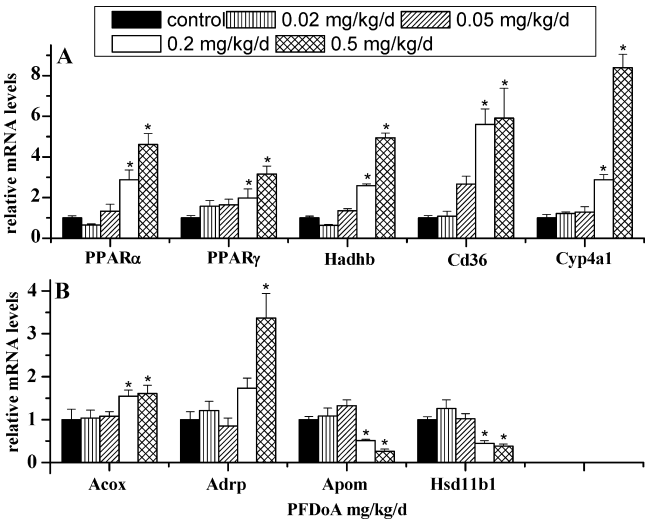

Figure 5. Real-time quantitative RT-PCR for hepatic mRNA expression levels of *PPARα, PPARγ, Hadhb, Cd36, Cyp4a1, Acox, Adrp, Apom* and *Hsd11b1* in control and PFDoA-exposed male rats. The values represent relative mRNA levels compared to the control group, which was set as 1. Asterisks (*) indicate statistically significant differences, $p < 0.05$.

endogenous fatty acids. Previous research indicated that PFOA exposure in rodents led to a number of changes that were typically associated with peroxisome proliferator chemicals, including increases in fatty acid β-oxidation enzymes and liver to body weight ratios.[11] The effects of PFOA on liver are assumed to be mediated by PPARα.[36] Similar to PFOA, PFDoA treatment resulted in marked biochemical changes associated with activation of the PPARα pathways, as well as pathways mediated by other nuclear receptors, such as CAR and PXR, which were involved in xenobiotic metabolism and include phase I, II, and III processes (Table S6 and S7, Supporting Information). These data elucidate how PPARs regulate target genes and lead to the aforementioned toxic end points, as well as the potential mechanism by which PFDoA causes hepatic steatosis (Figure 6), however, the PPARα-independent pathways altered by PFDoA should not be discounted until their functional significance regarding liver effects is better understood.

Following PPARα activation, biogenesis factors (*Pex11a* and *Pex14*) involved in the fission of peroxisomes were induced. As a consequence, peroxisome proliferation and fatty acid metabolism were enhanced in the liver.[37] Another consequence of PPARα activation is the coordinated induction of hepatic genes involved in the β-oxidation of fatty acids. Impaired fatty acid degradation, which involves upregulation of the *Acox1*, *Slc25a20*, *Decr2*, *Ech1*, *Hadhb*, *Acadv1*, *Acadm*, *Acadl*, *Ehhadh*, *Abhd1*, and *Gcdh* (GenMAPP pathways) genes, can also affect lipid metabolism and result in severe liver damage. Acetate is an end product of fatty acid oxidation, and the increased levels of both acetate and ketone bodies (3-HB and acetoacetate) following PFDoA treatment at the two highest dosages also reflect the consequences of PFDoA-induced lipid peroxidation. Our results also demonstrate that PFDoA induced reactive oxygen species (ROS), such as H_2O_2 and O_2^-, and significantly increased superoxide dismutase (SOD) activity and the production of thiobarbituric acid-reactive substances (TBARS) in the 0.5-dosed group (data not shown). These results suggest that PFDoA exposure may result in ROS production in the rat liver, perhaps by enhancing fatty acid β-oxidation, which may result in alterations in SOD, as well as lipid peroxidation levels. Being consistent with the changes in 3-HB and acetoacetate, genes involved in the synthesis and degradation of ketone bodies (HMG-CoA cycle), including *Hmgcs2* and *Acat1*, were significantly activated after PFDoA exposure (GenMAPP pathway). However, genes encoding the key enzymes that involved in cholesterol biosynthesis did not show any changes, and the serum cholesterol level remained unchanged, differing from the serum cholesterol-lowering effect of PFOA and PFOS.[38] Therefore, the toxic effect of PFDoA in cholesterol metabolism may differ from those of PFOA and PFOS, probably because PFDoA has a longer carbon chain.

The expression of *Cte1*and *Mte1* were induced 260.2- and 9.1-fold, respectively. The acyl-CoA thioesterases are key regulators of the homeostasis between free fatty acid and coenzyme A-conjugated fatty acids, and thus are important regulators of fatty acid metabolism.[39] When the levels of cumulative PFDoA are high in rat livers, *Cte1* is rapidly induced and could potentially supply the necessary ligand for PPARα. PPARα-regulated genes, including *Cte1*, would then be activated. *Cte1* would be further upregulated, and this cycle of events may amplify the PPARα signaling pathway.[39] Another factor involved in fatty acid accumulation is the induction of fatty acid biosynthesis pathways. *Fads2*, *Acaa2* and *Decr1*, which participated in mitochondrial fatty acid biosynthesis, were all consistently upregulated echoed with an elevation of lipids in liver tissue. Upregulation of *Cyp4a1*, *Cyp4a3*, and *Cyp2j4* induced by PPARα is consistent with the metabolic enhancement of unsaturated fatty acids, such as the arachidonic acid metabolic process. Increases in fatty acid synthesis and the subsequent elevation in TG and increased synthesis of other lipids lead to liver steatosis. Interestingly, the expression of genes encoding components of fatty acid biosynthesis and degradation are both significantly stimulated in rat liver following PFDoA exposure. These data are not only consistent with the observed accumulation of liver TG and steatosis, but also suggest that there is a net energy expenditure between the stimulated rates of fatty acid synthesis and oxidation.[38] Such a futile cycle and disruption of carbohydrate metabolism indicated that PFDoA significantly disturbs energy metabolism.

There are two major sources of hepatic lipids apart from the above-mentioned *de novo* fatty acid synthesis and lipogenesis including circulating free fatty acids (FFAs), which can be converted to triglycerides, especially when intrahepatic PFCAs are in excess.[40] Global microarray analysis showed that PFDoA-dosed induced noticeable expression of rat hepatic *Cd36*, a shared target of LXR, PXR and PPARγ, which comprised the lipid homeostasis mediation network.[41,42] Therefore, the increased levels of fatty acids and triglycerides in liver tissue and the opposite trend in blood serum most likely resulted from the induction of PPARγ and subsequent activation of *Cd36*, which facilitates increased uptake affinity for free fatty acids from the circulation to the liver tissue resulting in liver steatosis (Figure 6).

Other possible causes are also likely for the PFDoA-induced unbalance in liver lipid metabolism. The increase in adipose differentiation-related protein (*Adrp*) expression enhances triglyceride storage and reduces secretion of triglycerides and VLDL by diverting fatty acids from the VLDL assembly pathway into cytosolic triglycerides.[43] *Adrp* also plays an important role in the accumulation of triglycerides in liver. Furthermore, GeneChip analysis demonstrated down-regulated liver *Apom* expression, which occurred soon after the reduction in serum

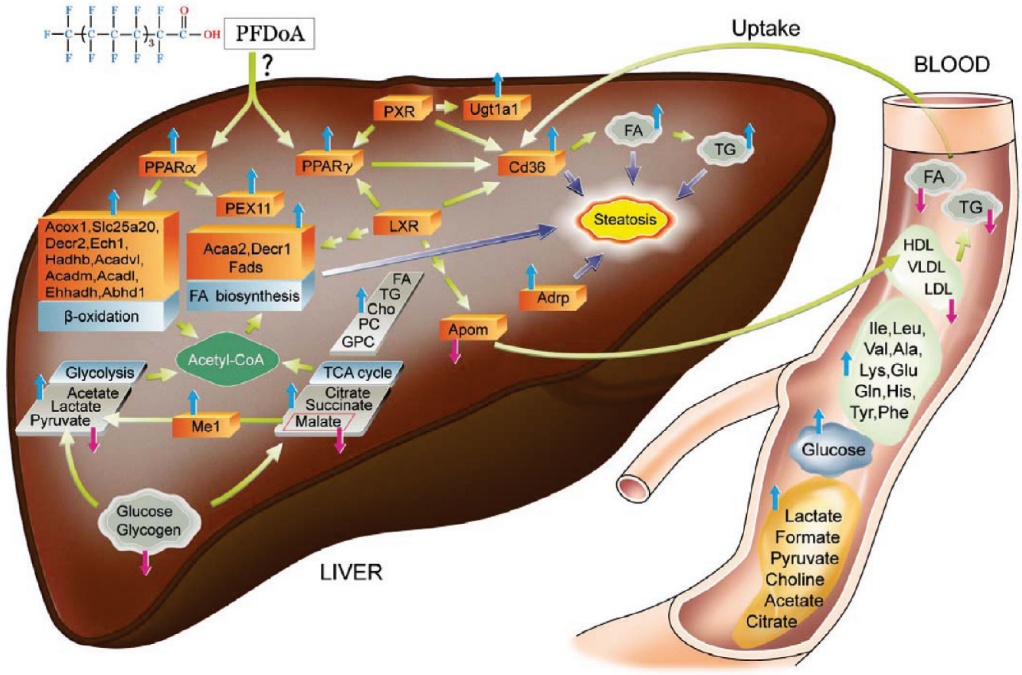

Figure 6. PPAR activation and subsequent alterations in hepatic gene expression involved in lipid homeostasis (fatty acid uptake, transport, biosynthesis, and β-oxidation), which leads to hepatic steatosis, induced by PFDoA exposure. Disturbed liver lipid and carbohydrate metabolism coupled with changes in serum metabolites reflects the PFDoA-induced toxicity in rat. FA, fatty acid; TG, triglyceride; PL, phospholipid; Cho, choline; PC, phosphorylcholine; GPC, glycerophosphorylcholine; LDL, low-density Lipoproteins; HDL, high-density lipoproteins; LDL, low-density lipoproteins; VLDL, very low-density lipoproteins. The orange panel represents the gene and the sky-blue panel represents the biological process. The gray rhombus denotes metabolites. The blue and mauve arrows represent increases and decreases in genes or metabolites, respectively. The indicated metabolic substances from rat serum were affected after PFDoA treatment.

lipoprotein. As *Apom* is mainly present in HDL, *Apom* may affect HDL metabolism, protect LDL against oxidation and more efficiently mediate cholesterol efflux.[44,45]

Increases in serum sugars, lactate, pyruvate, acetate, and creatine in dosed groups suggested changes in carbohydrate and energy metabolism after PFDoA treatment. In liver tissue extracts, decreased levels of glucose and pyruvate were accompanied by increased lactate and TCA cycle intermediates, indicating perturbed energy metabolism. Microarray analysis demonstrated that PFDoA directly or indirectly affected the expression of some key enzymes involved in carbohydrate metabolism and resulted in liver damage by interfering with the TCA process and glycolysis. Malic enzyme (*Me1*), a key enzyme that links the glycolytic pathway to the TCA cycle, catalyzes the reversible oxidative decarboxylation of malate to pyruvate.[46] Therefore, the high level of *Me1* expression in the liver was consistent with the decreased level of malate. Furthermore, the enhanced expression of solute carrier family 3 (*Slc3a*) and aconitase 1 (*Aco1*) contributed to the disturbances in carbohydrate and energy metabolism pathways caused by PFDoA exposure. The variety of amino acids affected by PFCAs has not been previously investigated, and metabonomics is a sensitive method for measuring fluctuations of these small molecules. The expression changes have also been observed in asparagine synthetase (*Asns*), histidine decarboxylase (*Hdc*), and phosphoserine aminotransferase 1 (*Psat1*), which are involved in asparagine, histidine, and aromatic amino acid synthesis, respectively. Therefore, the induction of these genes may be responsible for the elevated biosynthesis of these amino acids and a subsequent increase in protein synthesis and liver weight.

Clear dose-dependence was observable for the changes some endogenous metabolites and dose−effect relationships are important for describing the toxicological effects of PFCAs. Elevated serum glucose, citrate, formate, valine and isoleucine, as well as decreased fatty acids and lipoproteins, have been found to be the potential descriptors of PFDoA exposure even though the dosage of 0.02 mg/kg/d PFDoA showed little effects on rat liver metabolism. Thus, such dosage may represent a threshold for significant toxic effects. The present investigation affords a more in-depth understanding of the modes of PFCA activity and provides guidance for future investigations. It has to be said that due to the current state of genomic knowledge, a number of genes showing significant expression changes in this study cannot be fully explained and extended efforts in gene function identification remain essential.

Conclusions

These observations and analyses indicate that PFDoA exposure has induced changes in the metabolic pathways and perturbations in gene expression. A focus on specific changes in gene expression and their association with particular metabolic effects is an effective method for deducing the mechanisms of PFDoA toxicity. The combination of genomics and metabonomics approaches provides a systemic view of the toxicological effect of PFCAs on the organism. Activation of a series of PPARs and the downstream gene cascade involved in lipid homeostasis and perturbations in carbohydrate, energy, and amino acid metabolism illustrates the possible toxicological mechanism of such compounds.

Acknowledgment. This work was funded by the National Natural Science Foundation of China (20837004 for J.D., and 20825520 for H.T., respectively) and we acknowledge partial financial supports from the National Basic Research Program of China (2009CB118804 for Y.W.). We also thank Mr. Hang Zhu of Wuhan Institute of Physics and Mathematics for modifying the MatLab scripts used for color-coding the coefficient plots.

Supporting Information Available: Experimental details, Tables S1−S7, and Figures S1−S3. This material is available free of charge via the Internet at http://pubs.acs.org.

References

(1) Prevedouros, K.; Cousins, I. T.; Buck, R. C.; Korzeniowski, S. H. *Environ. Sci. Technol.* **2006**, *40*, 32–44.
(2) Apelberg, B.; Goldman, L.; Calafat, A.; Herbstman, J.; Kuklenyik, Z.; Heidler, J.; Needham, L.; Halden, R.; Witter, F. *Environ. Sci. Technol.* **2007**, *41*, 3891–3897.
(3) Guruge, K. S.; Taniyasu, S.; Yamashita, N.; Wijeratna, S.; Mohotti, K. M.; Senevriatne, H. R.; Kannan, K.; Yamanaka, N.; Miyazaki, S. *J. Environ. Monit.* **2005**, *7*, 371–377.
(4) Martin, J. W.; Smithwick, M. M.; Braune, B. M.; Hoekstra, P. F.; Muir, D. C.; Marbury, S. A. *Environ. Sci. Technol.* **2004**, *38*, 373–380.
(5) Taniyasu, S.; Kannan, K.; Horii, Y.; Hanari, N.; Yamashita, N. *Environ. Sci. Technol.* **2003**, *37*, 2634–2639.
(6) Betts, K. S. *Health. Perspect.* **2007**, *115*, 250–256.
(7) Kudo, N.; Suzuki-Nakajima, E.; Mitsumoto, A.; Kawashima, Y. *Biol. Pharm. Bull.* **2006**, *29*, 1952–1957.
(8) Kudo, N.; Suzuki, E.; Katakura, M.; Ohmori, K.; Noshiro, R.; Kawashima, Y. *Chem. Biol. Interact.* **2001**, *134*, 203–216.
(9) Ohmori, K.; Kudo, N.; Katayama, K.; Kawashima, Y. *Toxicology* **2003**, *184*, 135–140.
(10) Kudo, N.; Kawashima, Y. *Toxicol. Sci.* **2003**, *28*, 49–57.
(11) Kennedy, G. L.; Butenhoff, J. L.; Olsen, G. W.; O'Connor, J. C.; Seacat, A. M.; Perkins, R. G.; Biegel, L. B.; Murphy, S. R.; Farrar, D. G. *Crit. Rev. Toxicol.* **2004**, *34*, 351–384.
(12) Lau, C.; Butenhoff, J. L.; Rogers, J. M. *Toxicol. Appl. Pharmacol.* **2004**, *198*, 231–241.
(13) Berthiaume, J.; Wallace, K. B. *Toxicol. Lett.* **2002**, *129*, 23–32.
(14) Kudo, N.; Iwase, Y.; Okayachi, H.; Yamakawa, Y.; Kawashima, Y. *Toxicol. Sci.* **2005**, *86*, 231–238.
(15) 3M Company. US EPA Administrative Record, 2002, AR-226−0956.
(16) Seacat, A. M.; Thomford, P. J.; Hansen, K. J.; Clemen, L. A.; Eldridge, S. R.; Elcombe, C. R.; Butenhoff, J. L. *Toxicology* **2003**, *183*, 117–131.
(17) Seacat, A. M.; Thomford, P. J.; Hansen, K. J.; Olsen, G. W.; Case, M. T.; Butenhoff, J. L. *Toxicol. Sci.* **2002**, *68*, 249–264.
(18) Permadi, H.; Lundgre, B.; Andesson, K.; Sundberg, C.; DePierre, J. W. *Xenobiotic* **1993**, *23*, 761–770.
(19) Zhang, H.; Shi, Z.; Liu, Y.; Wei, Y.; Dai, J. *Toxicol. Appl. Pharmacol.* **2008**, *227*, 16–25.
(20) Lindon, J. C.; Holmes, E.; Nicholson, J. K. *FEBS. J.* **2007**, *274*, 1140–1151.
(21) Nicholson, J. K.; Lindon, J. C.; Holmes, E. *Xenobiotica* **1999**, *29*, 1181–1189.
(22) Nicholson, J. K.; Wilson, I. D. *Prog. Drug Res.* **1987**, *31*, 427–479.
(23) Bundy, J. G.; Spurgeon, D. J.; Svendsen, C.; Hankard, P. K.; Weeks, J. M.; Osborn, D.; Lindon, J. C.; Nicholson, J. K. *Ecotoxicology* **2004**, *13*, 797–806.
(24) Romero, R.; Espinoza, J.; Gotsch, F.; Kusanovic, J. P.; Friel, L. A.; Erez, O.; Mazaki-Tovi, S.; Than, N. G.; Hassan, S.; Tromp, G. *BJOG* **2006**, *113*, 118–135.
(25) Shi, Z.; Zhang, H.; Liu, Y.; Xu, M.; Dai, J. *Toxicol. Sci.* **2007**, *98*, 206–215.
(26) Nagayama, K.; Kumar, A.; Wuthrich, K.; Ernst, R. R. *J. Magn. Reson.* **1980**, *40*, 321–334.
(27) Bax, A.; Davis, D. G. *J. Magn. Reson.* **1985**, *65*, 355–360.
(28) Aue, W. P.; Karhan, J.; Ernst, R. R. *J. Chem. Phys.* **1976**, *64*, 4226–4227.
(29) Trygg, J. *J. Chemometr.* **2002**, *16*, 283–293.
(30) Martin, F. P.; Dumas, M. E.; Wang, Y.; Legido-Quigley, C.; Yap, I. K.; Tang, H.; Zirah, S.; Murphy, G. M.; Cloarec, O.; Lindon, J. C.; Sprenger, N.; Fay, L. B.; Kochhar, S.; van Bladeren, P.; Holmes, E.; Nicholson, J. K. *Mol. Syst. Biol.* **2007**, *3*, 112.
(31) Pfaffl, M. W. *Nucleic Acids Res.* **2001**, *29*, 2002–2007.
(32) Nicholson, J. K.; Foxall, P. J.; Spraul, M.; Farrant, R. D.; Lindon, J. C. *Anal. Chem.* **1995**, *67*, 793–811.
(33) Yap, I. K.; Clayton, T. A.; Tang, H.; Everett, J. R.; Hanton, G.; Provost, J. P.; Le Net, J. L.; Charuel, C.; Lindon, J. C.; Nicholson, J. K. *J. Proteome Res.* **2006**, *5*, 2675–2684.
(34) Coen, M.; Lenz, E. M.; Nicholson, J. K.; Wilson, I. D.; Pognan, F.; Lindon, J. C. *Chem. Res. Toxicol.* **2003**, *16*, 295–303.
(35) Kliewer, S. A.; Umesono, K.; Noonan, D. J.; Heyman, R. A.; Evans, R. M. *Nature* **1992**, *358*, 771–774.
(36) Rosen, M. B.; Lee, J. S.; Ren, H.; Vallanat, B.; Liu, J.; Waalkes, M. P.; Abbott, B. D.; Lau, C.; Corton, J. C. *Toxicol. Sci.* **2008**, *103*, 46–56.
(37) Shimizu, M.; Akter, M. H.; Emi, Y.; Sato, R.; Yamaguchi, T.; Hirose, F.; Osumi, T. *J. Biochem.* **2006**, *139*, 563–573.
(38) Bjork, J. A.; Lau, C.; Chang, S. C.; Butenhoff, J. L.; Wallace, K. B. *Toxicology* **2008**, *251*, 8–20.
(39) Hunt, M. C.; Lindquist, P. J.; Peters, J. M.; Gonzalez, F. J.; Diczfalusy, U.; Alexson, S. E. *J. Lipid Res.* **2002**, *41*, 814–823.
(40) Bradbury, M. W. *Am. J. Physiol. Gastrointest. Liver Physiol.* **2006**, *290*, 194–198.
(41) Lee, J. H.; Zhou, J.; Xie, W. *Mol. Pharm.* **2008**, *5*, 60–66.
(42) Febbraio, M.; Silverstein, R. L. *Int. J. Biochem. Cell Biol.* **2007**, *39*, 2012–2030.
(43) Magnusson, B.; Asp, L.; Boström, P.; Ruiz, M.; Stillemark-Billton, P.; Lindén, D.; Borén, J.; Olofsson, S. O. *Arterioscler. Thromb. Vasc. Biol.* **2006**, *26*, 1566–1571.
(44) Christoffersen, C.; Dahlbäck, B.; Nielsen, L. B. *Scand. J. Clin. Lab. Invest.* **2006**, *66*, 631–637.
(45) Venteclef, N.; Haroniti, A.; Tousaint, J. J.; Talianidis, I.; Delerive, P. *J. Biol. Chem.* **2008**, *283*, 3694–3701.
(46) Qian, S.; Mumick, S.; Nizner, P.; Tota, M. R.; Menetski, J.; Reitman, M. L.; Macneil, D. J. *Basic. Clin. Pharmacol. Toxicol.* **2008**, *103*, 36–42.
(47) Cloarec, O.; Dumas, M. E.; Trygg, J.; Craig, A.; Barton, R. H.; Lindon, J. C.; Nicholson, J. K.; Holmes, E. *Anal. Chem.* **2005**, *77*, 517–526.

PR9000256